Langmuir

Article

pubs.acs.org/Langmuir

Terms of Use

Adsorption of Mixtures of Poly(amidoamine) Dendrimers and Sodium Dodecyl Sulfate at the Air−Water Interface

Marianna Yanez Arteta,*[,†] Richard A. Campbell,[‡] and Tommy Nylander[†]

[†]Department of Physical Chemistry, Lund University, P.O. Box 124, S-221 00 Lund, Sweden

[‡]Institut Laue-Langevin, 6 rue Jules Horowitz, BP 156, 38042 Grenoble Cedex 9, France

ABSTRACT: We relate the adsorption from mixtures of well-defined poly(amidoamine) (PAMAM) dendrimers of generations 4 and 8 with sodium dodecyl sulfate (SDS) at the air−water interface to the bulk solution properties. The anionic surfactant shows strong attractive interactions with the cationic dendrimers at pH 7, and electrophoretic mobility measurements indicate that the association is primarily driven by electrostatic interactions. Optical density measurements highlight the lack of colloidal stability of the formed bulk aggregates at compositions close to charge neutrality, the time scale of which is dependent on the dendrimer generation. Adsorption at the air−water interface was followed from samples immediately after mixing using a combination of surface tension, neutron reflectometry, and ellipsometry measurements. In the phase separation region for dendrimers of generation 4, we observed high surface tension corresponding to a depleted surfactant solution but only when the aggregates carried an excess of surfactant. Interestingly, these depleted adsorption layers contained spontaneously adsorbed macroscopic aggregates, and these embedded particles do not rearrange to spread monomeric material at the interface. These findings are discussed in relation to the interfacial properties of mixtures involving dendrimers of generation 8 as well as polydisperse linear and hyperbranched polyelectrolytes where there is polyelectrolyte bound to a surfactant monolayer. The results presented here demonstrate the capability of dendrimers to sequester anionic surfactants in a controllable manner, with potential applications as demulsification and antifoaming agents.

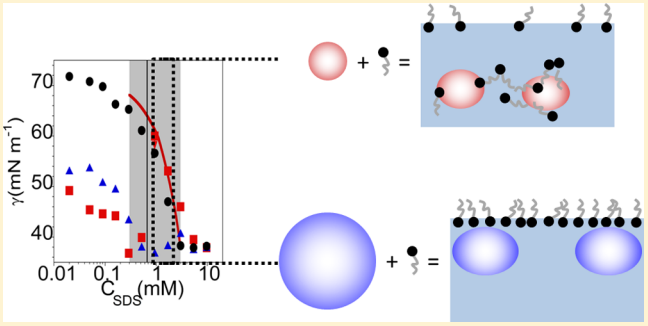

INTRODUCTION

Interactions in oppositely charged polyelectrolyte/surfactant (P/S) mixtures have been investigated extensively due to their important roles in consumer products, e.g., paints, detergents, drug formulations and foodstuffs, among others.[1] In many of these applications, the interfacial behavior of the mixtures determines their performance, but in spite of extensive studies, the mechanisms are not yet fully understood due to the complexity of these systems. Quite a number of different parameters control the interfacial behavior, such as the hydrophobicity and charge of the interface, the chain length of the surfactant,[2] and the polymer molecular weight and architecture,[3] among others. Furthermore, the interfacial behavior of P/S mixtures has been related to dynamic changes in the bulk phase behavior, both at the solid−liquid[4,5] and air−liquid[6,7] interfaces.

Oppositely charged P/S mixtures show strong attractive interactions in solution. The binding of the surfactant to the polyelectrolyte results in associative phase separation at bulk compositions close to charge neutrality of the complexes where the colloidal stability of the formed complexes is lowest.[8] The association in the phase separation region often shows large kinetic effects where aggregates are trapped in nonequilibrium states, and therefore, the protocols of mixing can be used to tune the sample properties.[9]

Several methods have been employed to study the interfacial behavior of the P/S mixtures, such as surface tensiometry, ellipsometry, and neutron reflectometry (NR), among others. While many polyelectrolytes have little or no affinity to the air−water interface, their presence in a surfactant solution synergistically enhances surfactant adsorption, even when no significant binding of the surfactant to the polymer in the bulk is observed.[10] Buckingham et al.[10] and Langevin et al.[2,11−13] described an interfacial structure where stretched linear polyelectrolyte chains that are oriented parallel to the surface are bound to the headgroups of a surfactant monolayer, and the polyelectrolyte counterions are expelled into the bulk.

Most of the studies on P/S mixtures at the air−water interface have used linear or polydisperse hyperbranched polyelectrolytes. In the latter category, a P/S mixture which has been extensively studied is poly(ethylene imine) (PEI) and SDS. The charge of PEI is pH-dependent, and thus, the interactions between PEI and SDS are stronger below neutral pH. Penfold et al.[3] reported that hyperbranched PEI with a low molecular weight forms multilayers at the air−water interface, while linear PEI and hyperbranched PEI of high molecular

Received: February 6, 2014
Revised: March 28, 2014
Published: April 30, 2014

   dx.doi.org/10.1021/la500473r | Langmuir 2014, 30, 5817−5828

weights exhibit only monolayer adsorption. Hyperbranched polymers have interesting properties, e.g., lower viscosity compared with that of their linear analogues, and they are therefore used in a range of commercial applications, e.g., detergents, adhesives, water treatment agents, and cosmetics.[14] They are usually synthesized by one-step self-polymerization, which reduces the cost but also makes them polydisperse with a less well-defined structure.[14] Thus, it can be challenging to rationalize their interfacial properties in a mixture with an oppositely charged surfactant.

The nonequilibrium nature of oppositely charged P/S systems, both in terms of the bulk and interfacial behavior, has been reported earlier for linear and branched polyelectrolytes.[6,7,15] For instance, kinetically trapped poly(diallyldimethylammonium chloride) (Pdadmac)/SDS aggregates formed close to charge neutrality can be deposited at the air−water interface.[6,16] For the PEI/SDS system, Tonigold et al.[17] showed that aggregates formed during the mixing process can become trapped in the interfacial layer close to charge equivalence. Also, Angus-Smyth et al.[18] found recently that aggregation of PEI/SDS complexes, which depends on the PEI charge, directly modified the dynamic interfacial properties of the mixtures.

Well-defined dendritic polyelectrolytes often show properties similar to those of their random hyperbranched analogues but have the advantage that the relationship between their structure and behavior in mixtures may be directly quantified rather than being related to the average properties. Dendrimers are formed by iterative sequence reactions which produce different generations that increase in size, molecular weight, and number of surface groups. The number of surface groups increases as a function of the generation (G) by 2^{G+2}.[19] Poly(amidoamine) (PAMAM) dendrimers,[20] which are the most studied type of dendritic polyelectrolyte, are constituted by a core of ethylendiamine and amidoamine branches with amine terminal groups, which have a pK_a between 8.0 and 9.2.[21] They are therefore positively charged at neutral pH, and the method of synthesis makes them highly monodisperse as they have a polydispersity index, M_w/M_n, of just 1.000002−1.005.[19] PAMAM dendrimers have been investigated as potential nanocarriers[22] as a result of their ability to host small hydrophobic or amphiphilic molecules in their interior. Other promising applications include gene vectors,[23,24] biosensors,[25] and water purification[26] and demulsification reagents.[27]

The interactions of PAMAM dendrimers with SDS have been studied previously in bulk solutions[28−30] and at the silica−water interface.[5] To our knowledge, however, a systematic study concerning the interactions of dendritic polyelectrolytes and amphiphiles at the air−water interfaces has not to date been carried out. The present study concerns the interactions of PAMAM dendrimers of generations 4 (G4) and 8 (G8) with SDS at the air−water interface with respect to the bulk solution properties. Our aim is to reveal the properties and behavior of monodisperse, hyperbranched P/S mixtures at the air−water interfaces with respect to the size of the polyelectrolyte and the phase behavior in the bulk. The bulk solution properties were characterized by electrophoretic mobility measurements to determine the charge of the P/S complexes formed in solution, and turbidity measurements to follow the dynamic changes in the bulk phase behavior. The surface properties of the mixtures immediately after mixing were investigated employing a combination of surface tensiometry to follow the adsorption behavior, NR with isotopic variation to characterize the structure and composition of the adsorbed layers, and ellipsometry to examine the influence of any aggregates that become embedded in the adsorption layers.

EXPERIMENTAL SECTION

Materials. All of the samples were prepared in deionized water, passed through a purification system (Milli-Q, resistivity = 18.2 mΩ·cm, and organic content = 4 ppb), and/or D2O (Euroiso-top, C. E. Saclay, France). Poly(amidoamine) dendrimers (PAMAM, Sigma-Aldrich) with ethylendiamine cores, of generations 4 (G4, 10 wt % in methanol) and 8 (G8, 5 wt % in methanol), were used without any further purification. Sodium chloride (NaCl, Suprapur 99.99%) was purchased from Merck and used as received. Aqueous solutions of 10 mM NaCl with pH adjusted to 7.2−7.4 by adding small volumes of concentrated hydrochloric acid (Merk, for analysis 37%) or sodium hydroxide (Sigma-Aldrich) were used as solvent. Hydrogenated sodium dodecyl sulfate (hSDS, BDH Chemicals Ltd. 99%) was recrystallized two times in ethanol (Kemetyl AB 99.5%). The purity was checked through surface tension measurements where no minimum in the surface tension versus concentration plot was observed. Deuterated SDS (dSDS, Cambridge Isotopes, 99%) was used as received.

Sample Preparation. All of the mixtures were prepared with the same mixing protocol. Solutions of the same volume of PAMAM and SDS were prepared with a concentration twice that of the intended final concentration, and they were poured simultaneously in a beaker. This procedure was used in order to minimize the concentration gradients during mixing.[9] In order to facilitate the comparison between the results for the two generations of dendrimers, we used the same total concentration of polymer charge, i.e., 100 ppm PAMAM-G4 and 108 ppm PAMAM-G8. Measurements were carried out at 23 ± 2 °C.

Electrophoretic Mobility Measurements. Electrophoretic mobility (EM) measurements were performed to obtain the charge of the PAMAM/SDS complexes in the mixtures. EM measurements were recorded using a zetasizer Nano ZS (Malvern Instruments Ltd., Worshestershire, UK). The electrophoretic mobility was measured using the M3-PALS technique (Phase analysis Light Scattering). The EM values of each sample correspond to the averages of 5 measurements.

Turbidity Measurements. The turbidity of the mixtures was determined by measuring the optical density at a wavelength of 450 nm (OD450). The absorbance values were recorded using a UV−visible spectrophotometer (Cary 300 BIO). The measurements were performed using a quartz Helma cell with a 10 mm path length. Each solution was measured immediately after mixing and 1 day, 2 days, 3 days, and 1 week after mixing. For each mixture, 40 mL of solution was prepared, approximately 3 mL was employed for the immediate mixtures, and the rest of the solution was separated in four different tubes (6 mL of solution in each tube), which were left until the measurements were performed. For the stored samples, 3 mL of the supernatant of the solutions was removed carefully to minimize the redispersion of any sedimented material.[7]

Surface Tension Measurements. The surface tension of the PAMAM/SDS mixtures was measured using a pendant drop tensiometer (Profile Analysis Tensiometer, PAT1, Sinterface Technologies, Berlin, Germany). The experimental setup and the principles of the technique have been described elsewhere.[31] A pendant drop of constant volume was formed at the tip of a stainless steel capillary of 2.0 mm diameter with an automated syringe pump. The surface tension of pure water was 72.7 ± 0.2 mN m^{-1}. The surface tension of the solutions was measured immediately after mixing until a plateau in the values was observed. For some dendrimer/SDS mixtures at low surfactant concentrations, the approach to steady state took several hours. Thus, in accordance with previous work for other P/S systems,[11] we defined steady state as when the surface tension change was less than 0.1 mN m^{-1}, i.e., the accuracy of the instrument, over a 10 min period.

NR Measurements. NR measurements were recorded on the time-of-flight reflectometer FIGARO at the Institut Laue-Langevin

dx.doi.org/10.1021/la500473r | Langmuir 2014, 30, 5817−5828

(Grenoble, France)[32] with a chopper pair giving neutron pulses with a wavelength resolution of 4% in the range 2−30 Å. Data acquisitions were carried out at fixed incident angles of 0.62°, 2.0°, and 3.8°. The specular reflectivity profiles presented are the intensity ratio of neutrons in the specular reflection, corrected for background scattering, to those in the incident beam as a function of the momentum transfer, Q, defined by

$$Q = \frac{4\pi \sin\theta}{\lambda} \quad (1)$$

where θ is the angle of incidence, and λ is the wavelength. The principles of the application of this technique at the air−water interface have been described elsewhere.[33] The measurements were performed at a planar air−water interface in PTFE troughs as described previously.[32] The solutions were prepared in two different isotopic contrasts of the surfactant, hSDS and dSDS, and two different isotopic contrasts of the solvent, D_2O (scattering length density of 6.36×10^{-6} Å^{-2}) and ACMW (air contrast matched water; a mixture of 8.1% by volume of D_2O in H_2O; a scattering length density of 0 Å^{-2}). The data were recorded in discrete time intervals until the reflectivity profiles had reached steady state, i.e., 1−8 h after mixing.

NR Data Evaluation. The NR data were modeled as stratified layers with the Abeles matrix method[34] using the software Motofit.[35] The contrasts fitted were PAMAM with dSDS/ACMW, hSDS/D_2O, and hSDS/ACMW. The parameters to fit for each layer were the thickness (d), the scattering length density (ρ), the material volume fraction (v), and the roughness (δ). The number of layers and composition of each layer depended on the system. The distance normal to the interface (d) in the volume fraction and scattering length density profile insets to the figures is defined as zero for the boundary between air and the first adsorbed layer when surface roughness is neglected. The scattering length density of the dendrimer and the surfactant in different solvent contrasts can be found in Table 1. The parameters reported correspond to the average of the ones obtained for the individual fitting of each contrast. The global fit function of Motofit was not employed for the corefinement of the data recorded in the different isotopic contrasts as the Q-range sensitive to the fitted structural parameters was different in each case, and thus small systematic errors in insensitive regions of the data unduly weighted the fits. The neutron reflectivity profiles of data recorded in each isotopic contrast were fitted individually employing the same model and equivalent parameters. The errors reported correspond to the standard deviation between the parameters of the different contrasts. The surface excess (Γ) of each compound was estimated through the following equation:

Table 1. Scattering Length Density of PAMAM Dendrimers in Different Solvents as well as the Corresponding Values for the Different Isotopic Contrasts of SDS[a]

material	PAMAM-G4 ACMW/D_2O	PAMAM-G8 ACMW/D_2O	hSDS	dSDS
ρ (10^{-6} Å^{-2})	1.3/2.2	1.5/2.5	0.4	6.8

[a]The scattering length densities were calculated based on the atomic composition, the scattering length, and the molecular volume. The scattering length density of the polymer in D_2O corresponds to an exchange of proton for deuteron on the primary amine groups.

$$\Gamma = \frac{d \cdot v \cdot \rho \cdot M}{b \cdot N_A} \quad (2)$$

where M and b represent the molar mass and scattering length of the component, respectively, and N_A is Avogadro's number.

Ellipsometry Measurements. Ellipsometry is an optical reflection technique used for the characterization of interfacial films. To analyze the reflection, polarized light is resolved into components in the plane of incidence (r_p) and in the normal of the plane of incidence (r_s). The reflection of linearly polarized light at an interface introduces a phase shift Δ between the two components, and changes the ratio of their amplitude by a factor tan Ψ.

$$\frac{r_p}{r_s} = \tan\Psi(\cos\Delta + i\sin\Delta) \quad (3)$$

The quantity Ψ is highly insensitive to the optical properties of thin, transparent films at the air−water interface, so only the measurements of Δ are presented. The effects on the measured ellipsometric phase shift of the surface layer (Δ_{surf}) is defined as follows:

$$\Delta_{surf} = \Delta_{P/S} - \Delta_0 \quad (4)$$

where $\Delta_{P/S}$ is the measured parameter for a P/S solution, and Δ_0 is the value for pure water. As the adsorption layers from PAMAM G4/SDS mixtures contain embedded macroscopic aggregates, they fall outside the thin film limit where the thickness of surface excess can be calculated. Therefore, the values of Δ_{surf} are used as an approximate representation of the total interfacial excess in the localized spot on the surface probed by the laser beam. The measurements were performed using an Optrel Multiskop null ellipsometer, with a Nd:YAG laser of wavelength of λ = 532 nm and an angle of incidence of 50°. The maximum data acquisition rate was ∼0.05 Hz. The instrument configuration employed has been described previously.[17] All of the samples were mixed immediately before measurement. The surface was aspirated for ∼3 s using a clean pipet tip attached to a water suction pump to remove any surface-trapped aggregates as well to create a fresh interface before the measurement.

RESULTS

PAMAM/SDS Interactions in the Bulk Solution. *Electrophoretic Mobility.* Figure 1 shows the electrophoretic mobility of the complexes measured immediately after mixing the components. The charge of the PAMAM/SDS complexes changes from positive to negative with increasing SDS concentration corresponding with previous reports on other oppositely charged P/S systems.[8] The point of charge neutrality corresponds to a concentration of 0.66 mM SDS for both systems where the primary amine concentration is 0.45 mM. An excess of SDS molecules in the bulk is needed to make the complexes neutral provided that only the primary amines are protonated. The ratio between the primary amine concentration and the SDS concentration is not unity as a result of the equilibrium between the adsorbed surfactant onto the polymer resulting in a finite free surfactant concentration at the point of charge neutrality. Although the association between oppositely

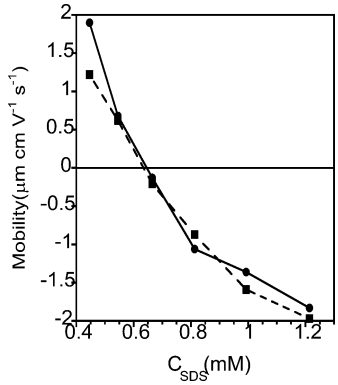

Figure 1. Electrophoretic mobility of PAMAM/SDS complexes for 100 ppm PAMAM-G4 (●) and 108 ppm PAMAM-G8 (■) as a function of the bulk SDS concentration in 10 mM NaCl. The lines are only to guide the eye. The data for PAMAM-G4/SDS are reproduced from ref 5.

dx.doi.org/10.1021/la500473r | Langmuir 2014, 30, 5817−5828

charged polyelectrolytes and surfactants is mainly electrostatic, the interactions are also influenced by the association of the surfactant hydrophobic tails. Factors such as the polyelectrolyte molecular flexibility and charge density and location can also influence the interactions with the surfactant.[36] The coincidence of the values for the different dendrimer generations shows that the number of primary amine groups controls the point of charge neutrality rather than the molecular weight. As such, the data suggest that the interaction is primarily controlled by electrostatic interactions under the conditions employed.

Turbidity. We now consider the aggregation of PAMAM/SDS complexes as a function of time after mixing. The turbidity of the mixtures for samples of both dendrimer generations was measured in terms of the optical density at a wavelength of 450 nm for samples immediately after mixing and after settling for 1 day, 2 days, 3 days, and 1 week (see Figure 2). A high optical density occurs due to the presence of P/S aggregates suspended in the solution; no absorption can be attributed to the dendrimer or the surfactant at this wavelength. Negligible turbidity is observed at bulk SDS concentrations below 0.2 mM and above 3 mM for the samples of both dendrimer generations studied, independent of the solution age. We attribute this observation to the complexes at bulk compositions far from the two-phase region having sufficient charge to hinder aggregation.

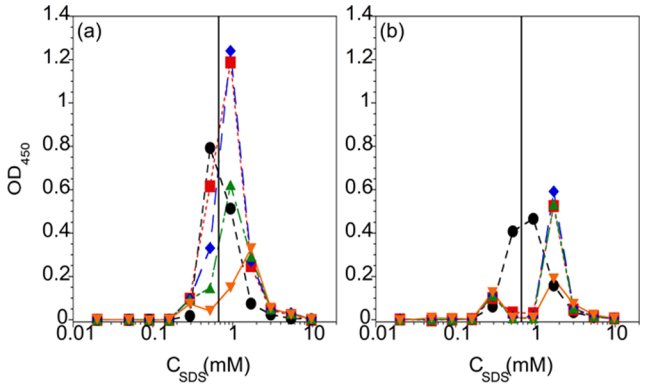

Figure 2. Optical density at 450 nm recorded using a UV−vis spectrophotometer to indicate the turbidity of PAMAM/SDS mixtures for (a) 100 ppm PAMAM-G4 and (b) 108 ppm PAMAM-G8 as a function of the bulk SDS concentration in 10 mM NaCl. The data was recorded immediately after mixing (black circles) and after settling for 1 day (red squares), 2 days (blue diamonds), 3 days (green triangles), and 1 week (orange inverted triangles). The vertical lines correspond to the concentration of charge neutrality of the complexes. The lines are only to guide the eye.

The maximum in the optical density for samples measured immediately after mixing occurs at surfactant concentrations close to the composition of charge neutrality for samples of dendrimers of both generations. The values decrease with time, which is attributed to the lack of colloidal stability of the aggregates, which consequently precipitate and sediment. The optical density for the PAMAM-G4/SDS mixtures around charge neutrality is initially much higher than that of the PAMAM-G8/SDS mixtures. Here, it should be borne in mind that the optical density is influenced by the size of the aggregates formed, the optical contrast between the particles and the solution, and the sedimentation rate.

Although the charges of the complexes are comparable, those involving the lower dendrimer generation show larger time-dependent effects in terms of stability compared to those involving the higher dendrimer generation. This difference points to the fact that the aggregation process and subsequently precipitation depend on the dendrimer generation, i.e., size, molecular weight, and number of surface groups of the dendrimer. An explanation could be linked to the relationship between the dendrimer generation and its density. Uppuluri et al. showed by molecular modeling and structural analysis studies that the outer surface of dendrimers of higher generation is denser.[37] Further, the dendrimers of higher generations also have a higher average density over the whole molecule,[38] which increases the probability that they form denser aggregates that will precipitate faster. Another explanation could be that differences in the structure of the complexes could cause PAMAM-G8/SDS complexes to form larger aggregates that sediment faster than PAMAM-G4/SDS. It has been proposed that low generation dendrimers interact with surfactant micelles without changing their structure, while higher generation dendrimers interact with more elongated or oblate micelles.[29,39] Similar behavior has been noticed for mixtures of cationic hydroxyethyl cellulose and SDS with different molecular weights, where a high molecular weight polymer forms larger aggregates that sediment faster.[40] It is possible than an interplay between these factors results in the observed differences in the dynamic changes of the sample turbidity for the two systems studied.

In accordance with our data, Wang et al.[41,42] have also reported strong binding of SDS to PAMAM-G3 at pH 7 as well as at more acidic pH. They observed that a 0.2 mM PAMAM-G3 solution (≈ 1380 ppm) at pH 7.4 became cloudy and precipitated at SDS concentrations higher than 2 mM yet was redispersed above 15 mM. The dendrimer concentration used was more than 10 times greater than that employed here, but the results from both studies are generally consistent.

For concentrations slightly above charge neutrality, the turbidity of the PAMAM-G4/SDS mixtures increases noticeably after 1 day and remains high for at least 2 days. A similar phenomenon has been observed for other polydisperse P/S mixtures.[7,15] In this case, the aggregates were considered not to be equilibrium structures but were formed as a result of concentration gradients during mixing and then became trapped in metastable states. Kinetically trapped aggregates formed at the edge of the phase separation region for oppositely charged, high molecular weight P/S systems have in some case been shown not to equilibrate on experimentally accessible time scales.[43]

The turbidity data have shown that freshly mixed samples are far from equilibrium in the phase separation region. This behavior is similar to that observed for other linear and/or less well-defined P/S systems such as Pdadmac/SDS,[7] NaPSS/DTAB,[15] and DNA/DTAB.[15] In each of these cases, it was shown that the surface tension data of the supernatant of well-equilibrated mixtures in the phase separation region could be modeled empirically as a depleted surfactant monolayer. Thus, it may be logical to assume that the interfacial layers formed by PAMAM/SDS mixtures that have been stored for several days are also depleted of the dendrimer. We therefore decided to perform the main study of the adsorption of PAMAM/SDS mixtures at the air−water interface immediately after mixing the components, so there is still a dispersion of small complexes and aggregates in solution and at the interface. This approach

dx.doi.org/10.1021/la500473r | *Langmuir* 2014, 30, 5817−5828

allows characterization of the adsorption layers when the dendrimer is still in a surface-active form for comparison with the influence of the dendrimer/surfactant aggregates on the interfacial layers.

PAMAM/SDS Interactions at the Air−Water Interface. *Surface Tension.* Figure 3 shows the surface tension values

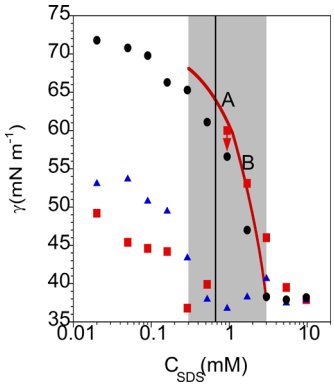

Figure 3. Surface tension of PAMAM/SDS mixtures for 100 ppm PAMAM-G4 (red squares) and 108 ppm PAMAM-G8 (blue triangles) and the predicted values for a depleted surface according to Ábraham et al.[15] (bold red line) as a function of the bulk SDS concentration in 10 mM NaCl. The data were recorded immediately after mixing. The vertical line corresponds to the concentration of charge neutrality of the complexes, and the gray area is the phase separation region. The red arrow indicates that the surface tension value had not reached steady state. The surface tension of pure SDS is also plotted for comparison (black circles).

recorded for fresh mixtures of PAMAM-G4 and PAMAM-G8 with SDS. Initially, the values are close to that of water, and a decrease with time occurs as the material adsorbs to the interface. The mixtures cause a synergistic lowering of the surface tension even at the lowest bulk surfactant concentrations measured (0.02 mM). Although the charge density is the same in the mixtures, the PAMAM-G4/SDS samples have a lower surface tension at low SDS concentrations than the PAMAM-G8/SDS samples. Asnacios et al.[2] found for polyacrylamide sulfonate and cationic surfactant mixtures that the polymer molecular weight did not influence the steady state surface tension but that the charge density did. However, they found a lower surface tension for the polymer with a higher charge density, contrary to what we observe for the dendrimers in the present study. It should be noted that Asnacios et al. rationalized their data with a model where one surfactant molecule in the surface monolayer is bound to each charge from the linear polyelectrolyte. This physical picture may not be valid in the case of PAMAM/SDS due to the bulky hyperbranched structure of the polyelectrolyte, which may explain the difference in behavior of the two systems.

The surface tension is generally low for samples in the phase separation region where there is a fine dispersion of PAMAM/SDS aggregates formed in the bulk. For PAMAM-G8/SDS mixtures, the values are also low at the higher surfactant concentrations in the phase separation region, while for PAMAM-G4/SDS mixtures there is a sharp increase in the surface tension for these samples which contain overcharged aggregates (points A and B). It was shown previously that a surface tension peak for the supernatant of well-equilibrated P/S mixtures in the phase separation region resulted from comprehensive precipitation of the polyelectrolyte with surfactant out of the liquid phase.[7,15] Employing the empirical model proposed recently by Ábraham et al.,[15] we calculated the expected surface tension values if the solution were fully depleted of dendrimer in the form of aggregates (bold red line in Figure 3). The calculated values agree very well with the measured experimental data in the peak region; thus, we might indeed expect that the air−water interface of these samples is depleted of dendrimer.

There are two reasons why this feature is very different from the peak in the surface tension that has been observed for other less well-defined P/S mixtures.[7,15] First, in the present work the peak is present for samples measured immediately after mixing the components, while the turbidity data show that the aggregates take several days to precipitate. However, previously the peak emerged only for samples where the changes in the bulk phase behavior had reached steady state. Second, in the present work the peak is positioned within the phase separation region. However, previously the peak coincided with the edge of the phase separation region that has the lowest surfactant concentration. A different mechanism is clearly at play. One explanation could be that the changes in surface tension are extremely slow, and thus, the values do not correspond to the steady state value. Point A (Figure 3) shows a very slow decrease in the surface tension values with time and does not reach steady state within several hours, as indicated by the red downward arrow. Nevertheless, it is still unclear why only overcharged PAMAM-G4/SDS and not positively charged PAMAM-G4/SDS complexes, nor any PAMAM-G8/SDS complexes, would immediately deplete the solution of surface-active material.

We note that the PAMAM-G4/SDS samples with negatively charged aggregates which exhibit the high surface tension values show an increase in turbidity between the moment of mixing and 1 day and that the turbidity remained high even after 1 week. To see if these changes in the state of bulk aggregation influence the surface tension, two PAMAM-G4/SDS mixtures in the peak region (both 1.7 mM SDS) were measured: one immediately after mixing and one after settling for 3 days (see Figure 4). The data from the two samples are equivalent. This result suggests that the high surface tension values of PAMAM-G4/SDS samples with negatively charged aggregates are independent of the ongoing aggregation process in the bulk. One explanation could be that all of the polyelectrolyte is

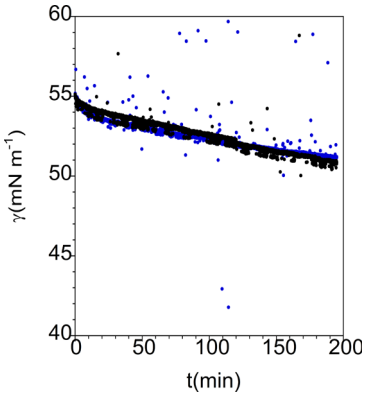

Figure 4. Decrease of surface tension with time is shown for PAMAM-G4/SDS mixtures with 100 ppm PAMAM-G4 and a bulk SDS concentration of 1.7 mM in 10 mM NaCl. The data were recorded immediately after mixing (black) and after settling for 3 days (blue).

dx.doi.org/10.1021/la500473r | *Langmuir* 2014, 30, 5817−5828

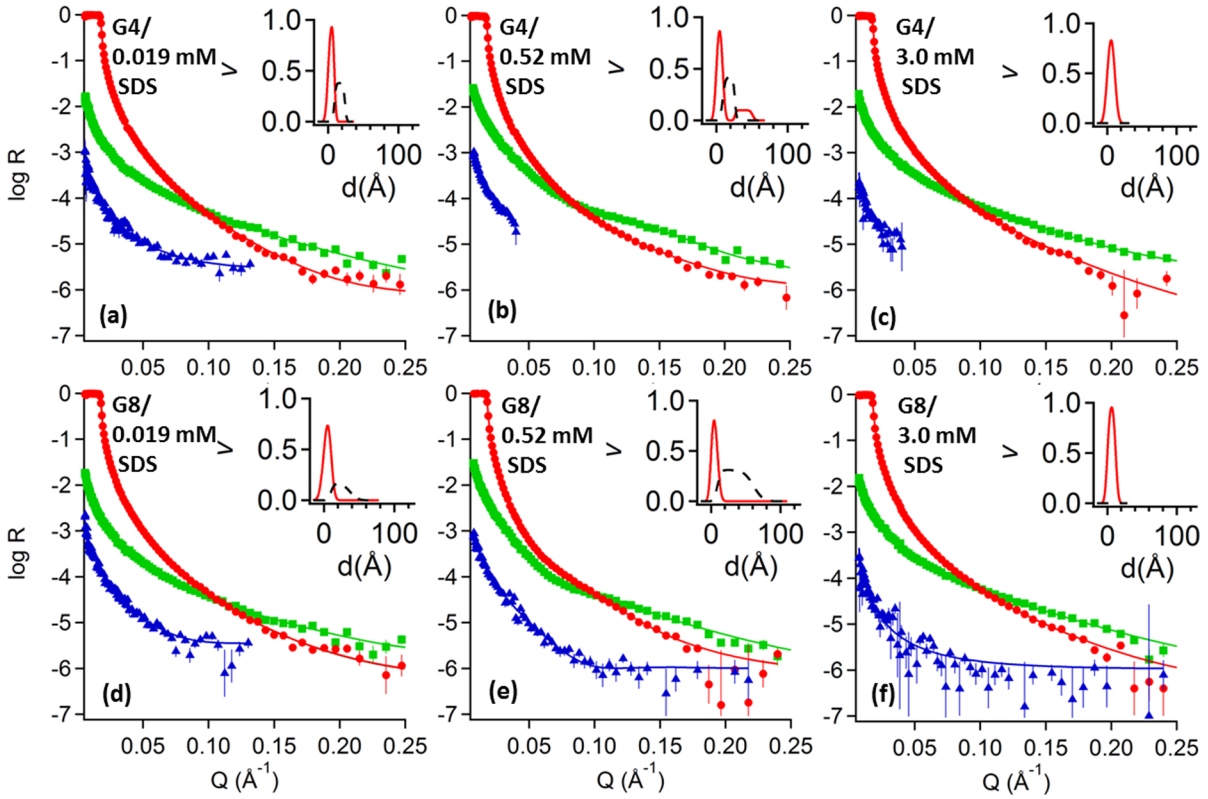

Figure 5. NR profiles for the adsorption at the air−water interface of PAMAM/SDS mixtures in 10 mM NaCl. The dendrimer generations were (a,b,c) 4 and (d,e,f) 8. The concentrations of SDS were (a,d) 0.019 mM, (b,e) 0.52 mM, and (c,f) 3.0 mM. The isotopic contrasts used to characterize the layers were PAMAM with dSDS/ACMW (green squares), hSDS/D_2O (red circles), and hSDS/ACMW (blue triangles). The lines correspond to the calculated models. The insets correspond to the volume fraction profiles (v) of PAMAM (black dashed line) and SDS (red line) as a function of the distance (d) to the interface.

Table 2. Parameters Obtained from the Modeling of the NR Profiles for the Adsorption of PAMAM-G4/SDS Mixtures at the Air−Water Interface

	surfactant layer			dendrimer layer				
C_{SDS} (mM)	d (Å)	δ (Å)	Γ (mg m^{-2})	d (Å)	ν	δ (Å)	Γ (mg m^{-2})	sub δ^a (Å)
0.019	9 ± 2	3 ± 2	1.1 ± 0.2	15 ± 1	0.38 ± 0.05	2 ± 1	0.7 ± 0.1	2 ± 2
0.090	9 ± 2	4 ± 2	1.1 ± 0.2	16 ± 2	0.41 ± 0.02	2 ± 1	0.8 ± 0.1	3 ± 2
0.16	10 ± 2	3 ± 2	1.2 ± 0.2	17 ± 3	0.40 ± 0.01	3 ± 1	0.8 ± 0.2	3 ± 2
0.52[b]	9 ± 2	3 ± 2	1.1 ± 0.2	17 ± 3	0.42 ± 0.07	3 ± 1	0.9 ± 0.3	3 ± 1
3.0	11 ± 2	4 ± 1	1.3 ± 0.2					4 ± 1

[a]Represents the roughness between the lowest layer and the solvent subphase. [b]The parameters for the second surfactant layer beneath the dendrimer layer were d = 25 ± 2 Å, ν = 0.10 ± 0.06, δ = 2 ± 1 Å, and Γ = 0.3 ± 0.2 mg m^{-2}.

present in aggregated form from the first moments of mixing and that the spreading of material at the interface from these aggregates is unfavorable, i.e., the material at the interface is a depleted surfactant monolayer with or without embedded macroscopic aggregates which do not reorganize to spread monomeric material on the time scale of the measurements. Ábrahám et al.[44] observed that aggregates of Pdadmac/SDS are collapsed only when they are overcharged. Therefore, we may speculate that compacted overcharged PAMAM-G4/SDS aggregates formed immediately after mixing deplete the bulk solution of surface-active small complexes and that even if they interact with the adsorption layer at the air−water interface they do not spread monomeric material to reduce its free energy; this situation is in contrast to the case for PAMAM-G8/SDS. The relationship between the surface tension and interfacial structure and morphology with respect to the dendrimer generation is clearly very complex and so is elaborated with reference to the NR and ellipsometry data. Gibb's equation is in practice impossible to apply to a multicomponent system as PAMAM/SDS mixtures for quantification as the activity coefficients of the surfactant and the polymer are modified due to bulk aggregation.[45] This limitation of surface tension analysis is indeed a primary driver for our application of neutron reflectometry to interfacial layers of PAMAM/SDS at the air−water interface as the structure and composition cannot be determined by laboratory-based methods such as surface tensiometry.

Neutron Reflectometry. We employed NR measurements on samples of different isotopic contrasts to determine the composition and the structure of adsorption layers of PAMAM-G4/SDS and PAMAM-G8/SDS mixtures at the air−water interface. The reflectivity profiles were successfully fitted using,

dx.doi.org/10.1021/la500473r | *Langmuir* 2014, 30, 5817−5828

Table 3. Parameters Obtained from the Modeling of the NR Profiles for the Adsorption of PAMAM-G8/SDS Mixtures at the Air−Water Interface

	surfactant layer			dendrimer layer				
C_{SDS} (mM)	d (Å)	δ (Å)	Γ (mg m^{-2})	d (Å)	ν	δ (Å)	Γ (mg m^{-2})	sub δ^a (Å)
0.019	10 ± 3	5 ± 1	1.2 ± 0.4	27 ± 5	0.17 ± 0.08	4 ± 1	0.6 ± 0.4	9 ± 4
0.090	9 ± 3	3 ± 2	1.1 ± 0.4	40 ± 5	0.19 ± 0.08	4 ± 1	0.9 ± 0.5	13 ± 5
0.16	10 ± 2	3 ± 2	1.2 ± 0.2	44 ± 6	0.22 ± 0.09	4 ± 1	1.2 ± 0.7	9 ± 4
0.52	9 ± 1	3 ± 1	1.1 ± 0.1	52 ± 6	0.31 ± 0.16	4 ± 1	2.0 ± 1.3	11 ± 4
0.94	9 ± 2	4 ± 3	1.1 ± 0.2	59 ± 8	0.30 ± 0.16	5 ± 2	2.2 ± 1.5	13 ± 3
1.7	9 ± 1	3 ± 2	1.1 ± 0.1	53 ± 9	0.08 ± 0.06	4 ± 1	0.5 ± 0.5	12 ± 5
3.0	12 ± 2	3 ± 1	1.4 ± 0.2					3 ± 2
9.7	11 ± 3	4 ± 2	1.3 ± 0.4					2 ± 1

[a]Represents the roughness between the lowest layer and the solvent subphase.

in most cases, a coadsorption model: an SDS monolayer at the air−water interface with a solvated dendrimer layer attached underneath to the surfactant headgroups. No penetration of the dendrimers into the surfactant monolayer was observed. For all of the samples studied, the dendrimer layer for both generations is highly compacted compared to the hydrodynamic diameter in solution, which is 49 Å for G4 and 133 Å for G8.[46] Figure 5 shows a selection of reflectivity profiles measured with their model fits, and Tables 2 and 3 list the fitting parameters obtained for all of the samples measured (5 bulk composition for G4 and 8 bulk composition for G8). We will now discuss the interfacial structure of the adsorption layers with respect to several different regions of bulk composition.

At the lowest SDS concentration measured (0.019 mM), the thickness and the coverage of the dendrimer layer (15 Å and 38% for G4; 27 Å and 17% for G8) are remarkably similar to that of pure adsorbed PAMAM monolayers at the silica−water interface (14 Å and 35% for G4; 33 Å and 16% for G8).[5] These data reveal that a similar force, the electrostatic attraction of cationic dendrimers to an oppositely charged surface which controls the adsorption to a planar hydrophilic silica surface, also controls the adsorption of the dendrimer molecules to the surface monolayer of oppositely charged surfactant. At the solid−liquid interface, the thickness and coverage of the pure dendrimer layers were attributed to the balance between the electrostatic attraction to the oppositely charged surface that caused deformation of the dendrimer structure and the lateral repulsion between dendrimer molecules. In the present work, at the air−water interface the PAMAM-G8 layer is thicker than that of PAMAM-G4 as a result of its inherent larger size, but the coverage is much lower, which we attribute to the larger electrostatic lateral repulsion between neighboring charged macromolecules of the higher generation. Because of the hyperbranched architecture of the dendrimer molecules and the interfacial structure revealed by NR, the SDS molecules in the monolayer at the air−water interface cannot neutralize all of the charges on the dendrimer molecules. This architecture prevents all of the charged groups synergistically interacting with surfactant molecules in the surface monolayer, which affects the surface tension. This physical picture is consistent with our interpretation of the converse dependence of surface tension trends on the molecular charge density between the PAMAM/SDS mixtures and linear P/S mixtures discussed above.

Table 4 shows some physical properties of the dendrimer: the molecular volume as reported previously,[5] the molecular area of the dendrimer (calculated assuming a spherical structure), and the area per surface group. If the surface area

Table 4. Physical Properties of Generations 4 and 8 of PAMAM Dendrimers

generation	surface groups	molecular volume (Å^3)	molecular surface area (Å^2)	area per charge (Å^2)
4	64	19 290	3480	54
8	1024	314 900	22 380	22

of SDS is taken as 25−40 Å^2, the area per charge of PAMAM-G4 in the bulk is larger than the molecular area of each surfactant molecule, while the area per charge of PAMAM-G8 is slightly lower. Note that the simple assumption that all of the primary amines are located on the periphery of the dendrimer is used in this calculation, even though some studies have shown that on larger generations, due to steric hindrance, some of the branches can be folded back inside the dendrimer molecule.[37] However, we can expect from previous results of dendrimer adsorption at the solid−liquid interface that the shape of the dendrimer is more compact at the air−water interface. The structure is better described as a half spheroid or a half ellipsoid, where two of the axes have the same longitude, a. Since they should spread equally distributed on the surface plane, the molecular volume of the dendrimer (V_M) may be given by

$$V_M = (1/2)4/3\pi \cdot d \cdot a^2 \quad (5)$$

where d represents the thickness of the dendrimer layer. Thus, it is possible to calculate the average cross-section of the dendrimer in contact with the surfactant monolayer: 1800 Å^2 for PAMAM-G4 and 11000 Å^2 for PAMAM-G8. Therefore, an average of <50% of the charges of the dendrimer is in proximity of the surfactant monolayer and therefore able to neutralize the SDS charges.

For intermediate bulk surfactant concentrations (0.52−1.7 mM), the thickness of the dendrimer layer and its volume fraction are both higher for G8 with a maximum around the SDS concentration corresponding to the charge neutrality of the complexes (0.66 mM; cf. Figure 1). This indicates the expansion of the G8 dendrimer monolayer due to the interaction with the surfactant. For G4 dendrimers within this range of SDS concentrations, both the thickness and surface excess is constant. Here, it should be noted that for the case of a preadsorbed monolayer of PAMAM dendrimer on silica, the addition of SDS caused expansion of the dendrimer layer due to the electrostatic binding and hydrophobic interactions. This increase in layer thickness was attributed to the lower effective charge on the dendrimer that leads to reduced electrostatic repulsion between neighboring macromolecules. At the air−

dx.doi.org/10.1021/la500473r | Langmuir 2014, 30, 5817−5828

water interface, SDS binds to the underside of the dendrimer layer only for the sample with an SDS concentration of 0.52 mM (closest to charge neutrality in the bulk) and only in the case of the generation 4 dendrimer. The surfactant layer thickness under the dendrimer layer is much larger than that of an SDS monolayer (25 ± 2 Å), which can be rationalized in terms of bound micelles or a bilayer-like structure. Although it may be intuitive to assume that the dendrimer and the surfactant will form a mixed layer at this concentration, fitting of data recorded in three isotopic contrasts shows clearly that no surfactant was found on the dendrimer layer. The surfactant layer beneath the PAMAM monolayer has a very low volume fraction of SDS (ν = 0.10 ± 0.06). The reason for forming this separated surfactant layer can be the high dendrimer coverage or possible repulsive interactions with surfactant monolayer at the air−water interface.

For the highest bulk SDS concentrations measured (3.0−9.7 mM), the NR data show that the interfacial structure comprises a surfactant monolayer at the air−water interface, and no dendrimer was found to bind to the headgroups of the SDS monolayer in these cases. We may infer that the dendrimer molecules are efficiently sequestered into negatively charged aggregates which do not preferentially interact with the free surface monolayer. We did not find it possible to fit the reflectivity profiles of PAMAM-G4/SDS mixtures with bulk surfactant concentrations of 0.94 or 1.7 mM to a consistent layer structure for the different isotopic contrasts recorded. For these samples, the rate by which the layer structure changed depended on the isotopic contrast. Figure 6 shows the evolution of reflectivity profiles for the isotopic contrast PAMAM-G4 with dSDS/ACMW as well as the other two isotopic contrasts recorded for samples with an SDS concentration of 1.7 mM. Uniquely for the data of the sample with dSDS/ACMW, the layer structure evolved from a pure SDS monolayer (d = 11 ± 2 Å) after 30 min, consistent with the other isotopic contrasts recorded, to one with additional material after 4 h, no longer consistent with the other data. It may be noted that this contrast is the one that is most sensitive to the total interfacial excess, and this time-dependent effect was not observed for any of the PAMAM-G8/SDS mixtures. The possible effects of aggregates directly penetrating the adsorption layers is not easy to detect with NR unless the concentration of aggregates is high, so complementary ellipsometry measurements were carried out to elucidate whether such aggregates penetrate the interface.

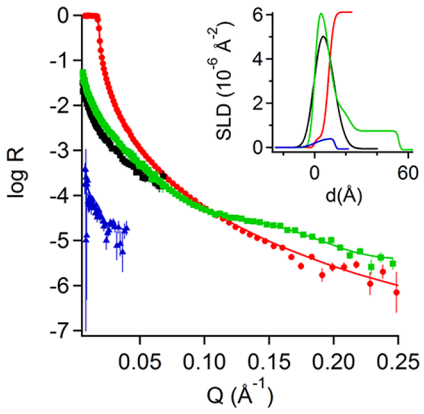

Figure 6. NR profiles for the adsorption at the air−water interface of the mixture PAMAM-G4/SDS with a bulk concentration of SDS of 1.7 mM in 10 mM NaCl. The isotopic contrasts used to characterize the layers involved dSDS/ACMW (green and black squares), hSDS/D_2O (red circles), and hSDS/ACMW (blue triangles). The data in black squares were recorded 30 min after mixing, while the rest of the data correspond to those over 4 h after mixing. The lines correspond to the calculated models. The insets correspond to the scattering length density profiles (SLD) as a function of the distance (d) to the air−water interface.

Ellipsometry. Ellipsometry measurements were performed on PAMAM-G4/SDS mixtures to see if there were any effects of aggregate penetration into the adsorption layers at the air−water interface. In this case, an increase in Δ_{surf} indicates a higher total interfacial excess, and any nonmonotonical response with time is related to lateral inhomogeneities on the micrometer scale. Figure 7 shows the kinetic evolution of Δ_{surf} for PAMAM-G4 mixtures with different bulk concentrations of SDS; for reference, an SDS monolayer under these measurement conditions gives a phase shift of Δ_{surf} = 0.9°.[17]

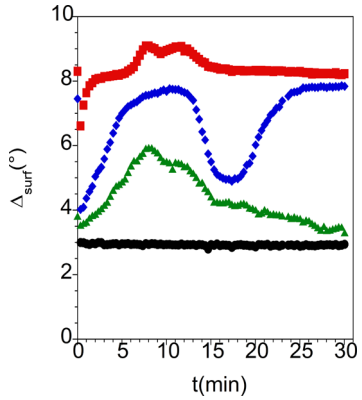

Figure 7. Ellipsometry angle Δ_{surf} versus time of PAMAM-G4/SDS mixtures for 100 ppm PAMAM-G4 and bulk SDS concentrations of 0.20 mM (black circles), 0.48 mM (red squares), 1.6 mM (blue diamonds), and 2.8 mM (green triangles) in 10 mM NaCl. The data were recorded immediately after mixing followed by cleaning of the surface by aspiration.

For the sample with the lowest bulk SDS concentration measured (0.20 mM), which is outside the phase separation region, there is no change in Δ_{surf} with time, which implies that to within the detection limit of the technique the film is laterally homogeneous. For the sample in the phase separation region with positively charged aggregates (0.48 mM), there is more material at the interface, which is consistent with the NR data where both the dendrimer and surfactant surface excesses are elevated. Also, the slight nonmonotonical response of Δ_{surf} with time shows that there is some lateral inhomogeneity from aggregates at the surface. For the sample in the phase separation region with overcharged aggregates (1.6 mM), the layers show large fluctuations, which we attribute to the presence of substantial amounts of aggregates embedded in the interfacial layer; the fluctuations are comparable in magnitude to those observed for PEI/SDS mixtures at high pH.[17] For the sample with the highest bulk SDS concentrations measured, which is at the edge of the phase separation region (2.8 mM), the value of Δ_{surf} increases until it reaches a maximum and then gradually decreases, again alluding to lateral inhomogeneity in the interfacial layer.

These measurements support our hypothesis above that the direct penetration of aggregates into the interfacial layers for

dx.doi.org/10.1021/la500473r | *Langmuir* 2014, 30, 5817−5828

samples in the phase separation region with negatively charged aggregates results in a larger total interfacial excess (as indicated by the kinetic dependences from NR; Figure 6) compared to that expected from a depleted surfactant solution (as is consistent with surface tension data; Figure 3).

DISCUSSION

The interactions of PAMAM dendrimers with SDS in the bulk solution and at the air−water interface are dependent on the bulk composition and the dendrimer generation. In addition, nonequilibrium effects due to the phase behavior of the system can have a significant impact on the interfacial properties, i.e., changes in the state of bulk aggregation with time affect the interfacial properties in a nonhomogeneous way. In the bulk solution, the main difference found between the mixtures involving the two dendrimer generations was that the phase separation process of the formation of macroscopic aggregates is slower for the PAMAM-G4/SDS system than for the PAMAM-G8/SDS system. This finding revealed that the aggregates formed have a very different density and/or structure, and this led to important implications on the interfacial layer structures and lateral morphologies formed.

We may now compare our results on the interactions of SDS with monodisperse hyperbranched PAMAM dendrimers with the interactions of surfactants with oppositely charged linear, polydisperse polyelectrolytes. The system Pdadmac/SDS exhibits a peak in its surface tension isotherm, which was originally rationalized in terms of the equilibrium competition of P/S complexes that have different surface activity.[47] Campbell et al. have since revealed the nonequilibrium nature of the system by demonstrating the influence of the sample handling method on the interfacial properties and by demonstrating experimentally that the peak is the result of the slow comprehensive precipitation of P/S aggregates out of the liquid phase;[7] an empirical model with no free fitting parameters to this effect has since been validated on data from three systems.[15] The PAMAM/SDS system also has a surface tension peak, but interestingly, it is present for freshly mixed samples and depends both on the dendrimer generation and on the charge of the aggregates. The interfacial structure of freshly mixed PAMAM-G4/SDS samples with negatively charged aggregates resembles that of a depleted surfactant monolayer with embedded macroscopic P/S aggregates. We make three conclusions. First, effectively all of the dendrimer molecules are sequestered into aggregates immediately after mixing, leaving no dendrimer to adsorb. Second, these aggregates penetrate the adsorption layer but do not rearrange to spread surface-active material at the interface; hence, the surface tension is high. Third, the behavior is not the same for PAMAM-G8/SDS mixtures where the surface tension values of freshly mixed samples are low throughout the phase separation region. It is not clear to us the underlying reasons why PAMAM-G8/SDS aggregates might spread at the air−water interface for freshly mixed samples yet PAMAM-G4/SDS aggregates do not, although this difference in behavior correlates with the slow dynamic changes in the bulk phase behavior, which is still far from equilibrium on the time scale of these measurements. We might expect that in time the surface tension of the samples with positively charged aggregates would converge to the predicted values in Figure 3 after the aggregates have fully precipitated in the bulk. A possible explanation for the low surface tension values for samples only with positively charged rather than negatively charged aggregates may be proposed: upon mixing of all samples the dendrimer is in a fully aggregated form, but only the positively charged aggregates interact readily with the oppositely charged headgroups of the surfactant monolayer and contribute to a reduction in the in surface tension through spreading monomeric material, while for samples with negatively charged aggregates the process is hindered. The more compacted structure of the negatively charged aggregates may also explain the difference in behaviors observed.

We may now compare our results to mixtures of polydisperse hyperbranched polyelectrolytes with oppositely charged surfactants. An example of a previously investigated, less well-defined hyperbranched polymer, which is commonly used in industrial applications, is PEI. Penfold et al.[3] have investigated the interactions between hyperbranched PEI of different molecular weights and SDS at the air−water interface for different solution pH values. The higher molecular weight PEI that they investigated was 25k, and thus, it is comparable with the 14k molecular weight of PAMAM-G4, while PAMAM-G8 has a molecular weight that is almost 10 times higher, 233k. For 25k PEI/SDS, the surface tension is pH-dependent, and at intermediate and high pH values (7 and 10, respectively), an initial sharp decrease in surface tension occurs at lower surfactant concentrations. This is followed by a plateau region and a small peak with increasing bulk SDS concentration, which is qualitatively similar to our data from freshly mixed PAMAM-G4/SDS samples in the phase separation region. It may be noted that the PEI/SDS measurements were carried out without added electrolyte, which explains why the phase separation region was found only over a narrow range of bulk SDS concentrations. At low bulk SDS concentrations, the NR data were consistent with a compact interfacial structure, similar to what we have observed for PAMAM-G4/SDS of similar bulk compositions. At intermediate bulk SDS concentrations, between 2 and 4 layers were required to describe the data NR data for PEI/SDS. The PAMAM-G4/SDS data from NR and ellipsometry revealed the adsorption of bulk aggregates for similar bulk compositions; this was not investigated for the PEI/SDS system. At high bulk SDS concentrations, the PEI/SDS layers had a compact interfacial structure similar to that of the layers formed from low bulk SDS concentrations but with a lower polymer volume fraction. Interestingly, no dendrimer was observed at the interface for the PAMAM-G4/SDS mixtures at equivalent bulk compositions.

Two other studies have focused on the interactions of high molecular weight hyperbranched PEI (750k) and SDS at the static[17] and dynamic[18] air−water interface with respect to the solution pH. For the static case, aggregates were found to be embedded in the adsorption layers, and this process was spontaneous at high pH, which was attributed to the lack of electrostatic repulsion that makes adsorption of aggregates favorable. In contrast, in the dynamic study it was found that there are stronger interactions of PEI and SDS at pH 4, which form more aggregates that reach the surface and collapse, spreading transient patches of the monolayer. We have not investigated the influence of pH on the adsorbed layers of PAMAM/SDS at the air−water interface, but we have observed that negatively charged PAMAM-G4/SDS aggregates do not spread material to the interface, which may not be the case for PAMAM-G8/SDS. The underlying reasons of why some aggregates spread monomeric material at the interface while others do not is clearly a subject which requires further work, but it has been proposed that factors such as the number

dx.doi.org/10.1021/la500473r | Langmuir 2014, 30, 5817−5828

density, structure, internal order, and/or hydrophobicity of the aggregates may be relevant.

A clear understanding of PAMAM/SDS interactions at interfaces is of critical importance for potential applications of dendrimers. As a result, previous work concerning the interfacial interactions from aqueous solutions of PAMAM dendrimers and single chain amphiphiles at interfaces was carried out on solid silica substrates. The extension of the knowledge toward the air−liquid interface helps, for example, to rationalize the use of dendrimers as vehicles for the delivery of amphiphilic drugs from a hydrophilic to a hydrophobic environment or vice versa. For example, it was found previously that PAMAM dendrimers of generations 1 to 3 can act as nanocontainers for the natural surfactants present in emulsions and that the demulsification efficiency increases with the dendrimer generation.[27] Therefore, the findings from the present work are also relevant to other applications of dendritic polyelectrolytes such as demulsification agents for the recovery of raw oil from oil−water emulsions. Through building on these findings, one could also imagine applications of dendrimers as antifoaming agents that sequester surfactants and hence reduce foaming. From the present work, we can infer that PAMAM-G4 could be a more efficient demulsification (or antifoaming) agent compared with PAMAM-G8, as negatively charged PAMAM-G4/SDS aggregates close to charge neutrality do not spread surface active material to the air−water interface, which is an important feature of this application.

CONCLUSIONS

The interactions between PAMAM dendrimers of generations 4 and 8 with SDS at the air−water interface are related to the molecular interaction and aggregation properties of the bulk solution. The dendrimers interact strongly with the oppositely charged surfactant and form complexes of different charge depending on the bulk composition. For the same molar concentration of amino groups, the concentration of anionic surfactant needed to form neutral complex with dendrimers is independent of the generation. This indicates that the interactions are mainly electrostatically driven. As for other P/S systems, PAMAM/SDS complexes with a low charge aggregate, and the aggregates flocculate with time resulting in precipitation due to their lack of colloidal stability. The time scale of the macroscopic changes in the bulk is dependent on the dendrimer generation: PAMAM-G8/SDS aggregates precipitate and sediment faster than PAMAM-G4/SDS aggregates. This difference in behavior has been discussed in terms of differences in the colloidal stability of the aggregates and/or differences in densities of the formed flocks.

We found that the interfacial behavior also depends on the bulk composition and the dendrimer generation by probing the surface structure, composition, and morphology of samples with three different interfacial techniques. For freshly mixed samples at low SDS concentrations, the presence of the dendrimer in solution enhances the surfactant adsorption. NR measurements show that the structure of the layers formed comprised an SDS monolayer with a compressed solvated dendrimer layer bound to the head groups. PAMAM interacts electrostatically with the surfactant monolayer, and the thickness and the composition of the dendrimer layer resemble that formed on oppositely charged solid substrates. Around the phase separation region, the properties of the adsorbed layers depend greatly on dendrimer generation, which correlates well with the bulk solution behavior. The surface tension of PAMAM-G8/SDS samples is low throughout the phase separation region, which is similar to that observed for other P/S mixtures with less well-defined polymers measured immediately after mixing. Freshly mixed PAMAM-G4/SDS mixtures, however, show an unusual behavior compared with that of other systems as the surface tension has a peak well inside the phase separation region. The data indicate that these samples are depleted of the dendrimer immediately after mixing the components, and this hypothesis was confirmed by NR measurements. Further, ellipsometry measurements showed that aggregates are embedded in the adsorption layers at the air/liquid interface. These aggregates clearly do not rearrange and spread surface-active material to the interface on experimentally accessible time scales. At very high SDS concentrations, no dendrimer bound to the surfactant monolayers was detected, showing the lack of surface activity of very negatively charged complexes.

Our findings have shown that the complexity of the interactions at hydrophobic interfaces of even a very well-defined P/S mixture depends greatly on variables such as the molecular weight and surface charge density of the dendrimer, and the state of aggregation in the bulk. As a result, this work can act as a basis for the development of potential applications of dendrimers and as a reference for understanding and optimizing the use of less well-defined mixtures used in everyday formulations.

AUTHOR INFORMATION

Corresponding Author

*E-mail: Marianna.Yanez@fkem1.lu.se.

Notes

The authors declare no competing financial interest.

ACKNOWLEDGMENTS

This work was supported by the Swedish Research Council (VR) through the Linnaeus Grant Organizing Molecular Matter (OMM) Center of Excellence (239-2009-6794). Knut and Alice Wallenberg's foundation funded the acquisition of the pendant drop tensiometer. We thank the ILL for the beam time allocation on FIGARO. We are also grateful to Karin Schillén, Imre Varga, and Bob Thomas for helpful discussions.

REFERENCES

(1) Holmberg, K.; Jönsson, B.; Krongberg, B.; Lindman, B. *Surfactants and Polymers in Aqueous Solution*, 2nd ed.; John Wiley & Sons, Ltd.: England, 2007; pp 299−302.

(2) Asnacios, A.; Langevin, D.; Argillier, J. F. Mixed monolayers of cationic surfactants and anionic polymers at the air-water interface: Surface tension and ellipsometry studies. *Eur. Phys. J. B* **1998**, *5* (4−6), 905−911.

(3) Penfold, J.; Tucker, I.; Thomas, R. K.; Zhang, J. Adsorption of polyelectrolyte/surfactant mixtures at the air−solution interface: poly(ethyleneimine)/sodium dodecyl sulfate. *Langmuir* **2005**, *21* (22), 10061−10073.

(4) Dedinaite, A.; Claesson, P. M.; Bergström, M. Polyelectrolyte−surfactant layers: adsorption of preformed aggregates versus adsorption of surfactant to preadsorbed polyelectrolyte. *Langmuir* **2000**, *16* (12), 5257−5266.

(5) Yanez Arteta, M.; Eltes, F.; Campbell, R. A.; Nylander, T. Interactions of PAMAM dendrimers with SDS at the solid−liquid interface. *Langmuir* **2013**, *29* (19), 5817−5831.

(6) Campbell, R. A.; Yanez Arteta, M.; Angus-Smyth, A.; Nylander, T.; Varga, I. Multilayers at interfaces of an oppositely charged

polyelectrolyte/surfactant system resulting from the transport of bulk aggregates under gravity. *J. Phys. Chem. B* **2012**, *116* (27), 7981−7990.
(7) Campbell, R. A.; Yanez Arteta, M.; Angus-Smyth, A.; Nylander, T.; Varga, I. Effects of bulk colloidal stability on adsorption layers of poly(diallyldimethylammonium chloride)/sodium dodecyl sulfate at the air−water interface studied by neutron reflectometry. *J. Phys. Chem. B* **2011**, *115* (51), 15202−15213.
(8) Goddard, E. D.; Hannan, R. B. Cationic polymer/anionic surfactant interactions. *J. Colloid Interface Sci.* **1976**, *55* (1), 73−79.
(9) Mezei, A.; Mészáros, R.; Varga, I.; Gilányi, T. Effect of mixing on the formation of complexes of hyperbranched cationic polyelectrolytes and anionic surfactants. *Langmuir* **2007**, *23* (8), 4237−4247.
(10) Buckingham, J. H.; Lucassen, J.; Hollway, F. Surface properties of mixed solutions of poly-l-lysine and sodium dodecyl sulfate: I. Equilibrium Surface Properties. *J. Colloid Interface Sci.* **1978**, *67* (3), 423−431.
(11) Asnacios, A.; Langevin, D.; Argillier, J.-F. Complexation of cationic surfactant and anionic polymer at the air−water interface. *Macromolecules* **1996**, *29* (23), 7412−7417.
(12) Stubenrauch, C.; Albouy, P.-A.; v. Klitzing, R.; Langevin, D. Polymer/surfactant complexes at the water/air interface: a surface tension and X-ray reflectivity study. *Langmuir* **2000**, *16* (7), 3206−3213.
(13) Ritacco, H.; Albouy, P.-A.; Bhattacharyya, A.; Langevin, D. Influence of the polymer backbone rigidity on polyelectrolyte-surfactant complexes at the air/water interface. *Phys. Chem. Chem. Phys.* **2000**, *2* (22), 5243−5251.
(14) Jikei, M.; Kakimoto, M.-A. Hyperbranched polymers: a promising new class of materials. *Prog. Polym. Sci.* **2001**, *26* (8), 1233−1285.
(15) Ábraham, Á.; Campbell, R. A.; Varga, I. New method to predict the surface tension of complex synthetic and biological polyelectrolyte/surfactant mixtures. *Langmuir* **2013**, *29* (37), 11554−11559.
(16) Noskov, B. A.; Grigoriev, D. O.; Lin, S. Y.; Loglio, G.; Miller, R. Dynamic surface properties of polyelectrolyte/surfactant adsorption films at the air/water interface: poly(diallyldimethylammonium chloride) and sodium dodecylsulfate. *Langmuir* **2007**, *23* (19), 9641−9651.
(17) Tonigold, K.; Varga, I.; Nylander, T.; Campbell, R. A. Effects of aggregates on mixed adsorption layers of poly(ethylene imine) and sodium dodecyl sulfate at the air/liquid interface. *Langmuir* **2009**, *25* (7), 4036−4046.
(18) Angus-Smyth, A.; Bain, C. D.; Varga, I.; Campbell, R. A. Effects of bulk aggregation on PEI-SDS monolayers at the dynamic air-liquid interface: depletion due to precipitation versus enrichment by a convection/spreading mechanism. *Soft Matter* **2013**, *9* (26), 6103−6117.
(19) Esfand, R.; Tomalia, D. A. Poly(amidoamine) (PAMAM) dendrimers: from biomimicry to drug delivery and biomedical applications. *Drug Discovery Today* **2001**, *6* (8), 427−436.
(20) Tomalia, D. A.; Baker, H.; Dewald, J.; Hall, M.; Kallos, G.; Martin, S.; Roeck, J.; Ryder, J.; Smith, P. A new class of polymers: starburst-dendritic macromolecules. *Polym. J.* **1985**, *17* (1), 117−132.
(21) Cakara, D.; Kleimann, J.; Borkovec, M. Microscopic protonation equilibria of poly(amidoamine) dendrimers from macroscopic titrations. *Macromolecules* **2003**, *36* (11), 4201−4207.
(22) Moorefield, C. N.; Newkome, G. R. Unimolecular micelles: supramolecular use of dendritic constructs to create versatile molecular containers. *C. R. Chim.* **2003**, *6* (8−10), 715−724.
(23) Kukowska-Latallo, J. F.; Chen, C.; Eichman, J.; Bielinska, A. U.; Baker, J. R., Jr. Enhancement of dendrimer-mediated transfection using synthetic lung surfactant exosurf neonatal in vitro. *Biochem. Biophys. Res. Commun.* **1999**, *264* (1), 253−261.
(24) Wang, Y.; Boros, P.; Liu, J.; Qin, L.; Bai, Y.; Bielinska, A. U.; Kukowska-Latallo, J. F.; Baker, J. R.; Bromberg, J. S. DNA/dendrimer complexes mediate gene transfer into murine cardiac transplants ex vivo. *Mol. Ther.* **2000**, *2* (6), 602−608.
(25) Shen, L.; Hu, N. Heme protein films with polyamidoamine dendrimer: direct electrochemistry and electrocatalysis. *Biochim. Biophys. Acta, Bioenerg.* **2004**, *1608* (1), 23−33.
(26) Chu, C.-C.; Ueno, N.; Imae, T. Solid-phase synthesis of amphiphilic dendron-surface-modified silica particles and their application toward water purification. *Chem. Mater.* **2008**, *20* (8), 2669−2676.
(27) Wang, J.; Li, C. Q.; Qu, H. J.; Hu, F. L.; Yang, Y. Terminal group effects on demulsification using dendrimers. *Pet. Sci. Technol.* **2010**, *28* (9), 883−891.
(28) Ottaviani, M.; Daddi, R.; Brustolon, M.; Turro, N.; Tomalia, D. Interaction between starburst dendrimers and SDS micelles studied by continuous-wave and pulsed electron spin resonances. *Appl. Magn. Reson.* **1997**, *13* (3), 347−363.
(29) Sidhu, J.; Bloor, D. M.; Couderc-Azouani, S.; Penfold, J.; Holzwarth, J. F.; Wyn-Jones, E. Interactions of poly(amidoamine) dendrimers with the surfactants SDS, DTAB, and C12EO6: an equilibrium and structural study using a SDS selective electrode, isothermal titration calorimetry, and small angle neutron scattering. *Langmuir* **2004**, *20* (21), 9320−9328.
(30) Fang, M.; Cheng, Y.; Zhang, J.; Wu, Q.; Hu, J.; Zhao, L.; Xu, T. New insights into interactions between dendrimers and surfactants. 4. Fast-exchange/slow-exchange transitions in the structure of dendrimer−surfactant aggregates. *J. Phys. Chem. B* **2010**, *114* (18), 6048−6055.
(31) Loglio, G.; Pandolfini, P.; Miller, R.; Makievski, A. V.; Ravera, F.; Ferrari, M.; Liggieri, L. Drop and Bubble Shape Analysis As a Tool for Dilational Rheological Studies of Interfacial Layers. In *Studies in Interface Science*; Möbius, D., Miller, R., Eds.; Elsevier: Amsterdam, 2001; Vol. *11*, pp 439−483.
(32) Campbell, R.; Wacklin, H.; Sutton, I.; Cubitt, R.; Fragneto, G. FIGARO: The new horizontal neutron reflectometer at the ILL. *Eur. Phys. J. Plus* **2011**, *126* (11), 1−22.
(33) Lu, J. R.; Thomas, R. K.; Penfold, J. Surfactant layers at the air/water interface: structure and composition. *Adv. Colloid Interface Sci.* **2000**, *84* (1−3), 143−304.
(34) Abeles, F. Sur la propagation des ondes electromagnetiques dans les milieux stratifies. *Ann. Phys.* **1948**, *3* (4), 504−520.
(35) Nelson, A. Co-refinement of multiple-contrast neutron/X-ray reflectivity data using MOTOFIT. *J. Appl. Crystallogr.* **2006**, *39* (2), 273−276.
(36) Goddard, E. D. Polymer—surfactant interaction part II. Polymer and surfactant of opposite charge. *Colloids Surf.* **1986**, *19* (2−3), 301−329.
(37) Uppuluri, S.; Keinath, S. E.; Tomalia, D. A.; Dvornic, P. R. Rheology of dendrimers. I. Newtonian flow behavior of medium and highly concentrated solutions of polyamidoamine (PAMAM) dendrimers in ethylenediamine (EDA) solvent. *Macromolecules* **1998**, *31* (14), 4498−4510.
(38) Betley, T. A.; Banaszak Holl, M. M.; Orr, B. G.; Swanson, D. R.; Tomalia, D. A.; Baker, J. R. Tapping mode atomic force microscopy investigation of poly(amidoamine) dendrimers: effects of substrate and pH on dendrimer deformation. *Langmuir* **2001**, *17* (9), 2768−2773.
(39) Ottaviani, M. F.; Andechaga, P.; Turro, N. J.; Tomalia, D. A. Model for the interactions between anionic dendrimers and cationic surfactants by means of the spin probe method. *J. Phys. Chem. B* **1997**, *101* (31), 6057−6065.
(40) Zhou, S.; Xu, C.; Wang, J.; Golas, P.; Batteas, J.; Kreeger, L. Phase behavior of cationic hydroxyethyl cellulose−sodium dodecyl sulfate mixtures: effects of molecular weight and ethylene oxide side chain length of polymers. *Langmuir* **2004**, *20* (20), 8482−8489.
(41) Wang, C.; Wyn-Jones, E.; Sidhu, J.; Tam, K. C. Supramolecular complex induced by the binding of sodium dodecyl sulfate to PAMAM dendrimers. *Langmuir* **2007**, *23* (4), 1635−1639.
(42) Wang, C.; Wyn-Jones, E.; Tam, K. C. Complexation between amine- and hydroxyl-terminated PAMAM dendrimers and sodium dodecyl sulfate. *Colloids Surf., A* **2010**, *364* (1−3), 49−54.
(43) Mészáros, R.; Thompson, L.; Bos, M.; Varga, I.; Gilányi, T. Interaction of sodium dodecyl sulfate with polyethyleneimine:

surfactant-induced polymer solution colloid dispersion transition. *Langmuir* **2003**, *19* (3), 609−615.
(44) Ábrahám, A.; Mezei, A.; Meszaros, R. The effect of salt on the association between linear cationic polyelectrolytes and sodium dodecyl sulfate. *Soft Matter* **2009**, *5* (19), 3718−3726.
(45) Purcell, I. P.; Lu, J. R.; Thomas, R. K.; Howe, A. M.; Penfold, J. Adsorption of sodium dodecyl sulfate at the surface of aqueous solutions of poly(vinylpyrrolidone) studied by neutron reflection. *Langmuir* **1998**, *14* (7), 1637−1645.
(46) Ainalem, M.-L.; Carnerup, A. M.; Janiak, J.; Alfredsson, V.; Nylander, T.; Schillen, K. Condensing DNA with poly(amido amine) dendrimers of different generations: means of controlling aggregate morphology. *Soft Matter* **2009**, *5* (11), 2310−2320.
(47) Bell, C. G.; Breward, C. J. W.; Howell, P. D.; Penfold, J.; Thomas, R. K. Macroscopic modeling of the surface tension of polymer−surfactant systems. *Langmuir* **2007**, *23* (11), 6042−6052.